Tracing Recent Large Herbivore Influence on Soil Carbon in Permafrost and Seasonally Frozen Arctic Ground Using Lipid Biomarkers: a Pilot Study

Torben Windirsch[1,2,*], Kai Mangelsdorf[3], Guido Grosse[1,2], Juliane Wolter[1,4], Loeka L. Jongejans[1,+], and Jens Strauss[1]

[1]Alfred Wegener Institute Helmholtz Centre for Polar and Marine Research, Permafrost Research Section, Potsdam, Germany
[2]University of Potsdam, Institute of Geosciences, Potsdam, Germany
[3]German Research Centre for Geosciences GFZ, Helmholtz Centre Potsdam, Organic Geochemistry Section Potsdam, Germany
[4]University of Potsdam, Institute of Biochemistry and Biology, Potsdam, Germany
[*]now at Research Institute for Sustainability Helmholtz Centre Potsdam (RIFS), Potsdam, Germany
[+]now at Ruhr-University Bochum, Institute of Geography, Bochum, Germany

Correspondence to: Torben Windirsch, torben.windirsch@awi.de

Abstract

This study investigates the impact of large herbivores on soil organic matter (OM) stability in Arctic permafrost and seasonally frozen ground ecosystems, focusing on the potential preservation effect of grazing. Soil samples were collected from Siberian and Finnish permafrost and non-permafrost areas and organic carbon content, carbon-to-nitrogen ratio, stable carbon isotopes as well as the content of *n*-alkanes and *n*-alcohols were analysed to assess OM stability. The results suggest that grazing activity, particularly in permafrost environments, preserves soil OM by reducing decomposition. Permafrost soils exhibit higher functionalized to non-functionalized biomarker ratios, indicating in general better preservation under frozen conditions. While differences in grazing intensities had minor effects, the data also showed variability due to soil heterogeneity, especially in seasonally frozen ground ecosystems. Nevertheless, there are slight trends towards enhanced OM preservation with increasing grazing intensity, especially in permafrost, emphasising the potential role of grazing in locally preserving Arctic soil OM. This pilot study offers initial insights into the impact of large herbivores on OM stability in cold-region ecosystems, suggesting that significant effects may require prolonged, intensive grazing pressure.

Key words: Arctic ecology, herbivory, carbon storage, permafrost, lipid biomarkers, soil organic matter, carbon quality

37

1 Introduction

Global warming is directly related to continuously rising carbon dioxide levels in the Earth's atmosphere (IPCC 2021). In addition to direct anthropogenic greenhouse gas emissions from fossil fuel burning, land ecosystem changes have been identified as a large source of emissions as soil organic carbon (OC) may become more vulnerable to mineralization (Kaplan *et al.* 2010). Large quantities of organic carbon are stored in soils and can partially be mobilised and mineralised to greenhouse gases by microbial activity following soil warming (van Groenigen *et al.* 2011) and surface erosion (Lal 2022). In order to assess the extent and physical context of this OC mobilisation, it is important to investigate the effects of land cover changes and environmental land use scenarios on the OC dynamic (Ramesh *et al.* 2019). A large portion of global soil organic carbon is found in the terrestrial Arctic (Hugelius *et al.* 2020, Strauss *et al.* 2021), with a large share currently still stored in permafrost (Schuur *et al.* 2015, 2022). Due to Arctic amplification, ongoing climate warming is leading to particularly strong warming in the Arctic (Previdi *et al.* 2021), resulting in permafrost warming and subsequently widespread and deeper thawing of soils (Bowen *et al.* 2020). As a consequence, an increasing portion of the organic matter (OM) stored in permafrost becomes bioavailable again for microbial decomposition, leading to the release of OC in the form of the greenhouse gases CO_2 and CH_4 (Turetsky *et al.* 2019, Bowen *et al.* 2020). In addition to OC, also other temperature-stabilised elemental soil components such as nitrogen (Strauss *et al.* 2022), various mineral components (Monhonval *et al.* 2021, Stimmler *et al.* 2023), or even contaminants like mercury (Schuster *et al.* 2018, Rutkowski *et al.* 2021) are affected by thaw mobilisation.

Land cover change can promote deepening of the active layer – the seasonally thawed soil on top of permafrost – and thus permafrost thaw by changing the permafrost insulating layer of the local vegetation and organic-rich soil cover, which has a strong impact on snow distribution, and by changing soil wetness and thus surface hydrology. For example, deforestation can cause deepening of the active layer and loss of soil carbon due to e.g. soil

66 exposure to solar radiation (Peplau *et al.* 2022), and shrubification can cause ground warming
67 via snow trapping, and therefore also active layer deepening (Mekonnen *et al.* 2021). Surface
68 disturbances, either natural or anthropogenic, can hereby affect soil carbon storage on short
69 or long time scales (Forbes *et al.* 2001, Grosse *et al.* 2011). In particular, permafrost can be
70 severely affected by wildfires via post-fire permafrost thaw (Jones *et al.* 2015, Zhang *et al.*
71 2023), which also affects soil carbon storage (Harden *et al.* 2006, Genet *et al.* 2013).
72 Anthropogenic-driven land use change, in particular the mentioned deforestation and
73 intensification of agricultural activities in some permafrost regions, can also have large effects
74 on permafrost thermal conditions, active layer deepening, and also soil carbon stability. Land
75 use pressure will likely increase further in the Arctic, as a result of changing climate and
76 therefore a poleward shift of usable agricultural zones (Bradley and Stein 2022, Ward Jones
77 *et al.* 2024). Some forms of land use might, however, help stabilising permafrost and therefore
78 soil carbon. A key to better understanding of the effects of natural and anthropogenic
79 landscape changes and landscape management on the greenhouse gas emission budget will
80 be the investigation of the soil organic carbon inventory. In addition to bulk carbon elemental
81 parameters (e.g. total organic carbon (TOC) and bulk carbon isotope signal ($\delta^{13}C$)), especially
82 the utilisation of lipid biomarkers extracted from the soils is a promising tool for revealing, along
83 with vegetational variations, changes in the decomposition state of the OM.
84
85 In particular, large-mammal herbivory has been hypothesised to influence soil OM composition
86 and stability for cold-region ecosystems (Olofsson and Post 2018, Ylänne *et al.* 2018,
87 Kristensen *et al.* 2022). Zimov *et al.* (1995) suggested that in the late-Pleistocene stable cold-
88 environment ecosystem, called the Mammoth steppe, the substantial presence of large
89 herbivorous animals had strong impact on the snow and vegetation conditions, resulting in
90 enhanced preservation of permafrost and soil OM. Large herbivores – browsing for food in
91 winter – trample, compress, and partially remove the insulating snow, which leads to more
92 effective contact between winter air and the ground and thus more intense soil cooling (Zimov
93 *et al.* 2009, Park *et al.* 2015, Beer *et al.* 2020). In addition, animal density results in varying

94 degrees of trampling damage and nutrient availability from animal faeces (Grellmann 2002,
95 Schuur *et al.* 2008), and selective grazing throughout the year results in vegetation changes
96 through food and habitat preferences. As these animal activities can reduce soil insulation
97 against low winter temperatures, they are thought to contribute to stabilising permafrost
98 conditions. In contrast, the vegetation shift from sturdy and shrubby tundra vegetation towards
99 graminoid-dominated landscapes reduces shadowing effects of vegetation in summer, leading
100 to increased summer soil warming. However, due to the substantially longer winters, these
101 less-insulated surfaces compensate for the slightly enhanced summer warming by enhanced
102 winter cooling, producing an annual net-negative soil temperature relative to a shrub-covered
103 surface. This is due to the fact that, unlike shrubs, graminoids tend to fall over underneath the
104 snow and do not form an insulating, air pocket-filled layer (Blok *et al.* 2010, Macias-Fauria *et*
105 *al.* 2020). Adding to this, graminoid-dominated vegetation is comparably light-coloured,
106 increasing the albedo and therefore reflection of energy from solar radiation. The cold ground
107 conditions, reinforced in that way in widespread permafrost regions during the late
108 Pleistocene, prevented OM from decomposition and continued accumulation of soil OM by
109 maintaining a frozen state with low microbial activity (Turetsky *et al.* 2019, Windirsch *et al.*
110 2022a).
111
112 Focusing on herbivory, previous studies (Windirsch *et al.* 2022a, Windirsch *et al.* 2023c)
113 examining the exact same sampling points as investigated in this study, but in regard to
114 sediment and OM characteristics, revealed that large herbivore activity likely reduces
115 permafrost thaw via aforementioned mechanisms, but has no significant effect on the amount
116 of carbon stored within the soil during the relatively short time the study sites had been
117 exposed to heavy grazing pressure (23 years on permafrost, 50 years on seasonally frozen
118 ground). In seasonally frozen ground, no clear trends for carbon storage increase along with
119 increasing grazing intensity were found (Windirsch *et al.* 2023c). In contrast to these studies,
120 we now worked towards deciphering the relation between grazing and OM degradational state
121 instead of total soil carbon storage. Therefore, we investigated in situ carbon quality - meant

as the degree of 'freshness' or 'state-of-decomposition' along grazing gradients. Our main research question is: how does the degradational state of soil OM vary in relation to the influence of large-mammal herbivory? In order to answer this, we investigated whether large herbivore activity at various grazing intensities alters biomarker signals of the soil OM, and whether biomarker signals are affected by the local thermal regime of the ground (i.e., permafrost vs. seasonally frozen ground). First, we analysed bulk total organic carbon (TOC) characteristics as well as functionalized (*n*-alcohols) versus non-functionalized (*n*-alkanes) biomarkers in sediment samples along grazing intensity transects. These lipid biomarkers provide semi-specific information on OM sources such as vegetation types, as well as on OM decomposition levels (Strauss *et al.* 2015, Jongejans *et al.* 2021). Secondly, we compared permafrost sites to study sites with seasonally frozen ground (SFG) to gain insights into the carbon storage processes in a warming Arctic where permafrost will increasingly transition to seasonally frozen ground. We hypothesise that under high grazing impact biomarker indices for degradation (Higher Plant Alcohol index (HPA) and Carbon Preference Index (CPI)) are higher compared to non-grazed sites with warmer soil conditions and therefore more degraded OM. Thirdly, we determined whether large herbivore grazing leads to reduced OM decomposition or increased OM input. We did this in a pilot study approach, collecting a set of samples with large spatial spread to capture different landscape and soil types, as well as different degrees of herbivore activity, to test if and under which circumstances significant effects can be found.

2 Study area

We collected soil samples from permafrost and non-permafrost sites from two terrestrial Arctic study areas that are exposed to a range of large-herbivore grazing intensities at the local scale.

The first study area is located in the continuous permafrost zone in the floodplains of the Kolyma River in northeastern Siberia, approximately 100 km inland from the Arctic Ocean (Fig. 1a) (Fuchs *et al.* 2021). The landscape is characterised by Yedoma permafrost deposits and

thermokarst lake basins (Palmtag *et al.* 2015, Veremeeva *et al.* 2021). The climate is continental with large temperature amplitudes (average of -33 °C in January; average of 12 °C in July) and low mean annual precipitation of less than 200 mm (Göckede *et al.* 2017), most of which usually falls in winter as snow. As a consequence, meltwater is the main water source for soil wetness in this region. Sediments are mainly silt-sized with additional clayish content, in drained thermokarst basins often topped with peat or peat-mixed sediment. Active layer depth ranges between 38 and 80 cm, depending on animal activity and vegetation type (Windirsch *et al.* 2022a). The drained thermokarst basins are covered by tussock grasses (*Carex appendiculata* (Trautv. & C.A.Mey.) Kük.) and short tundra vegetation (dwarf-shrub dominated with *Betula nana*, *Empetrum nigrum* and *Vaccinium* and *Salix* species being common), following wetness gradients from seasonally flooded areas to snowmelt affected areas. Wet areas feature tall grasses such as *Calamagrostis canadensis* (Michx.) P. Beauv: var. *langsdorfii* (Link) Inman (Corradi *et al.* 2005). On the surrounding uplands, tundra vegetation, interspersed with willow shrubs, is found.

The second study area, featuring seasonally frozen ground, is located in the glacially imprinted area of northern Finland (Fig. 1b and c) (Windirsch *et al.* 2021a, Windirsch *et al.* 2023c). In this area, glacial sands provide the main substrate for the formation of shallow podzols on top of glacial gravel and debris deposits. Relief mainly consists of glacial features such as eskers and moraines (Paoli *et al.* 2018). In depressions, peat mires formed on top of the sandy material. *Pinus sylvestris* Linné and *Betula pubescens* ssp. *tortuosa* (Ledeb.) N.I.Orlova Nyman form vast forests in which wetlands covered by typical tundra vegetation and graminoids form more open areas. Underneath, bryophytes and ground lichen form the lowermost vegetation layer in this area (Oksanen and Virtanen 1995, Maliniemi *et al.* 2018). A subarctic and continental climate provides an annual air temperature amplitude of approximately 26 °C in humid conditions (Finnish Meteorological Institute 2021).

While these study areas differ in many aspects, such as the presence of permafrost, soil parent material (peat, sandy and silty mineral soil), glacial history and herbivore assembly, they also share traits we consider vital for this study. Vegetation types are similar (graminoid-dominated,

dwarf-shrub dominated, occasionally larger shrubs or trees) and provide similar functions to the soil, regarding their insulating properties, even though they are not identical species-wise. Also, the grazing intensities exerted by large herbivorous animals are comparable animal-density-wise. In both areas, the top soil is frozen for parts of the year, hence reducing decomposition processes during this time. Further, both areas are high-latitude and do not experience direct industrial impacts. Since this study looks into grazing pressure-related, and therefore also thermal regime-related decomposition proxies in soil OM, vegetation, grazing pressure and the frozen state of the top soil are the most relevant aspects. To identify effects on degradation caused by permafrost, we consider the active layer of permafrost sites separately, comparing them to the also seasonally frozen top soil samples from our non-permafrost study area in the following.

3 Methods

3.1 Sampling approach

We collected the soil samples for lipid biomarker extraction during field campaigns in northeastern Siberia (2019) (Windirsch *et al.* 2022a) and northern Finland (2020 and 2022) (Windirsch *et al.* 2023c) (Fig. 1). The exact coordinates of all sampling locations are reported in the datasets available on the PANGAEA repository (Windirsch *et al.* 2021b, Windirsch *et al.* 2022b; c). During these campaigns, we sampled transects along gradients of large-mammal grazing intensity (including trampling effects and in general, animal presence and activity), spanning across five identified grazing intensities (Fig. 1). In each study area, several transects, each within a single landform or soil type, were selected, covering exclosure sites (3 sites in total), occasional seasonal migration routes (rare grazing; 3 sites in total), daily migration routes (seasonal in Finland) (occasional grazing; 6 sites in total), high-frequency seasonal daily migration routes (regular grazing; 3 sites in total), and pasture or supplementary feeding sites (pastures; 7 sites in total). These intensities are based on manipulation, such as fences around exclosures and across the landscape to guide migration or seasonal supplementary feeding, and long-term observation by research station staff, combined with

our own observations for several days in the beginning of each sampling campaign. For final site selection, we also used dung abundance and the animal-induced shift in vegetation composition to identify the intensity of animal activity. In Siberia, the intermediate intensities 'rare' and 'regular' were omitted as identification was unclear. This sampling approach was applied in a pilot study design, capturing a large variety of soil and vegetation types as well as landscape forms but not having a balanced set of sampling sites. Also, due to limited resources and the objective to test our methods for finding differences between grazing intensities at all, we did not take any replicate samples, though we collected dung samples as a reference for the pure animal signal. A list of all sampling sites is provided in table 1.

In Siberia, we sampled permafrost-affected soils and the active layer in three sites along a transect in a partially drained thermokarst basin (sites B) with increasing grazing intensity towards the basin centre, as well as two sites along a transect on the surrounding Yedoma uplands (sites U) in the Pleistocene Park experimental area (68.51 °N, 161.50 °E) (Zimov 2005). The local herbivore species are Yakutian horses (*Equus ferus caballus* Linné), Kalmykian cows (*Bos primigenius taurus* Linné), sheep (*Ovis* sp. Linné), reindeer (*Rangifer tarandus tarandus* Linné), musk oxen (*Ovibos moschatus* Zimmermann), yaks (*Bos mutus* Przewalski), moose (*Alces alces* Linné), European bisons (*Bos bonasus* Linné) and American bisons (*Bos bison* Linné), which access the pasture sites year-round.

In Finland, we sampled a series of locations at the Kutuharju Field Research Station (69.15 °N, 27.00 °E) in a forest tundra area in a glacially imprinted landscape. The glacial retreat from these surfaces was estimated to 9,700 cal yr BP (Stroeven *et al.* 2016). The sample series consists of 8 mineral soil sites (M) and 10 peat sites (P) which seasonally freeze from the surface in winter, but are not underlain by permafrost. In addition, three reference sites outside the managed station area were sampled during this campaign, which we identified as grazing intensity 3 (migration routes with occasional grazing, representing the natural or most common state in northern Finland). There, we sampled a mineral soil, a peatland soil, and a peat soil

underneath a birch forest to cover the predominant landscape types. The predominant large herbivore species in this area is reindeer, along with moose.

For comparison to the soil sample contents, we took a fresh faecal sample of the predominant herbivore species in each study area. In Siberia, we sampled fresh horse dung at the location U5. In Finland, we took a sample of fresh reindeer dung at site S-2M.

We sampled a total of 23 sites, with either one core or one soil profile each, reaching depths between 11 and 176 cm. From the material collected, we selected 58 subsamples for biomarker analysis. In frozen ground, we obtained soil cores using a SIPRE permafrost auger (Jon's Machine Shop, Alaska). In unfrozen peat soils, we used a peat corer (Eijkelkamp), and in unfrozen mineral soils we sampled within a soil profile using fixed-volume stainless steel cylinders. Frozen cores were transported intact to the labs, where they were subsampled for biomarker analysis, while unfrozen material was subsampled directly in the field. To avoid contamination with fresh vegetation material, the uppermost sections that held living plant roots from the soil cores and soil profiles were excluded. For the lower sections, we specifically sampled visibly separable stratigraphic units and the freeze-thaw interface, if visible.
Biomarker samples were taken exclusively using metal instruments and transported in sterile and annealed glass jar sample containers. The samples were frozen directly after sampling at -20° C and kept frozen until further laboratory analysis started.

3.2 Laboratory analysis

All samples were freeze-dried using a Zirbus Sublimator 15. After drying, the samples were powdered and homogenised using a Fritsch Pulverisette 5 mill equipped with corundum jars. For lipid biomarker extraction, we followed the procedures presented by Jongejans *et al.* (2021). Lipids were extracted from approximately 5 g of the homogenised samples using accelerated solvent extraction (ASE) with dichloromethane / methanol (DCM / MeOH 99:1 v/v) using a ThermoFisher Scientific Dionex ASE 350. The samples were each held in a static

phase (5 min heating) for 20 min (75 °C, 5 MPa). Samples were subsequently concentrated using a Genevac SP Scientific Rocket Synergy evaporator at 42 °C.

We added internal standards for compound quantification: 5α-androstane as a reference for *n*-alkanes and 5α-androstan-17-one for *n*-alcohols. After removal of the asphaltenes (*n*-hexane-insoluble fraction) by asphaltene precipitation, we separated the resulting maltene fraction (*n*-hexane soluble compounds) by medium pressure liquid chromatography (MPLC) (Radke *et al.* 1980) into aliphatic, aromatic and NSO (nitrogen, sulphur, and oxygen containing) components using *n*-hexane. The NSO fraction was additionally separated into an acidic and neutral polar compound fraction. For this, each NSO fraction was transferred to an potassium hydroxide impregnated silica column where the acidic components were trapped as their potassium salts and the neutral polar components were washed through. Afterwards, the potassium salts were protonated again using DCM / formic acid (98:2 v/v) and the acidic fraction was washed off the column. Before measurements, the neutral polar fraction (containing the alcohols) was silyllated by adding 100 µl DCM / MSTFA (N-Methyl-N-(trimethylsilyl)trifluoroacetamide; 50:50 v/v) and heating the samples at 75 °C for one hour.

n-Alkanes from the aliphatic fraction as well as n-alcohols from the NSO fraction were measured using a Thermo Scientific ISQ 7000 Single Quadrupole Mass Spectrometer equipped with a Thermo Scientific Trace 1310 Gas Chromatograph (capillary column from BPX5, 2 mm x 50 m, 0.25 mm) as used by Jongejans *et al.* (2018), measuring with a MS transfer line temperature of 320 °C and an ion source temperature of 300 °C with an ionisation energy of 70 eV at 50 µA. Compound identification and quantification in relation to the internal standards from full-scan mass spectra (*m*/*z* 50-600 Da, 2.5 scans s^{-1}) were carried out using the software Xcalibur.

In addition, we analysed the samples for total organic carbon content (TOC), using an Elementar soliTOC cube analyser, and total nitrogen (TN), using an Elementar rapidMAX N analyser. From these measurements we calculated the TOC to TN (C/N) ratio.

We measured bulk stable carbon isotope ratios ($\delta^{13}C$) after removing carbonates from our samples, using hydrochloric acid at 50 °C for three hours. The samples were measured with a Delta V Advantage Isotope Ratio MS supplement equipped with a Flash 2000 Organic Elemental Analyser, and results are provided in ‰ relative to the Vienna Pee Dee Belemnite (VPDB) standard (Coplen *et al.* 2006). Both C/N ratio and $\delta^{13}C$ ratio can be used as an indication for the quality and source of OM (Biester *et al.* 2014, Strauss *et al.* 2015). In fresh organic-rich samples, microbial activity is the main factor for OM decomposition, and the microorganisms prefer the consumption of ^{12}C over ^{13}C, which leads to higher $\delta^{13}C$ values of the remaining OM (Golubtsov *et al.* 2022). However, in recently deposited OM, the source of the OM, produced from different vegetation types, has a strong impact on the $\delta^{13}C$ signature variation, complicating the use of this parameter as a decomposition indicator (Wynn 2007).

3.3 Lipid biomarker indices

Three indices from the measured lipid concentrations were calculated: (1) the average chain length (ACL) of *n*-alkanes with *i* carbon numbers as a measure of the dominating chain length distribution (Poynter and Eglinton 1990), providing information on the respective OM sources, (2) the carbon preference index (CPI) of *n*-alkanes as a measure of the OM degradation level (Bray and Evans 1961, Marzi *et al.* 1993) and (3) the higher-plant alcohol index (HPA) as a measure of leaf wax component degradation (Poynter 1989) applying the following equations:

(Eq. 1) $$ACL_{23-33} = \frac{\Sigma\, i\, C_i}{\Sigma\, C_i}$$

(Eq. 2) $$CPI_{23-33} = \frac{\Sigma\, odd\, C_{23-31} + \Sigma\, odd\, C_{25-33}}{2 * \Sigma\, even\, C_{24-32}}$$

(Eq. 3) $$HPA = \frac{\Sigma\, (alcohols\, C24, C26, C28)}{\Sigma\, (alcohols\, C24, C26, C28) + \Sigma\, (n{-}alkanes\, C27, C29, C31)}$$

following the methods applied by Jongejans *et al.* (2021). Lower CPIs indicate a higher degradation state of OM (Glombitza *et al.* 2009, Strauss *et al.* 2015). The same holds true for lower HPA values (Poynter 1989). High HPA values express a high content of *n*-alcohols vs.

316 *n*-alkanes, and thus of functionalized to non-functionalized biomarkers. During decomposition
317 it is suggested that aliphatic functionalized biomarkers are degraded to non-functionalized
318 aliphatics (Poynter 1989). However, in fresh OM both parameters are affected by the
319 biomarker composition of the initial source material (Jongejans *et al.* 2020, 2021). Thus, to
320 use these parameters to assess different degradation stages, the initial source material should
321 be comparable.
322
323 **3.4 Statistics**
324 We tested for statistical significance of the differences in all parameters. Due to independence
325 of our samples, when separated by grazing intensity and therefore location, and unequal
326 sample amounts within the groups, we chose to run a Kruskal-Wallis H test. We did this in the
327 R environment using the 'stats' package (R Core Team 2021) and used a confidence level of
328 0.95. Therefore, if the resulting *p*-value is smaller than 0.05, the differences are statistically
329 significant.
330 We further run mixed effect models in the R environment ('lme4' package) for the biomarker
331 indices, using 'grazing intensity' as a fixed variable and 'site' as a random variable to identify
332 random effects between sites, accounting for the spatial heterogeneity of the analysed soils.
333 Positive random interception values indicate that the respective biomarker index baseline
334 value at one site is higher than the overall baseline, while negative values indicate the
335 opposite.
336
337 **4 Results**
338 Here, we report the TOC, C/N, $\delta^{13}C$, $ACL_{23\text{-}33}$ (for *n*-alkane chain lengths with 23 to 33 carbon
339 atoms), $CPI_{23\text{-}33}$ (for *n*-alkane chain lengths with 23 to 33 carbon atoms), total *n*-alkane
340 concentration and HPA values for all permafrost-affected and seasonally frozen ground
341 samples. We distinguish between the seasonally thawed samples (top 38 cm of all study sites;
342 Fig. 2) and the full sampling depth from all sites (Fig. 3). All data will be published in
343 PANGAEA. Missing values for C/N ratio are due to very low TN values below the instrument

detection limit of 0.1 wt%. In the following, all samples are referred to by using the site name and the mean sample depth.

4.1 TOC

In permafrost-affected samples TOC ranges between 0.81 wt% (CH19-B1 26.25 cm bs) and 21.13 wt% (CH19-B3 71.5 cm bs) with a mean value of 7.53 wt%. For seasonally frozen ground, the TOC range is between 0.42 wt% (FI20-S-2M 18.5 cm bs) and 53.99 wt% (FI20-S-4P 82.5 cm bs) with a mean of 28.54 wt%. There are no general trends with depth across sites visible (Fig. S1). Many TOC values are in the same range for the permafrost and seasonally frozen ground samples, with exception of the peat samples from seasonally frozen ground showing much higher TOC values, similar to the reference dung samples with 37.66 wt% (horse, Siberia) and 44.69 wt% (reindeer, Finland). When comparing grazing intensities, values are lowest in exclosure samples and seem to increase towards pastures at least at the permafrost sites (Fig. 2).

4.2 C/N ratio

For the permafrost-affected samples, C/N values range from 11.40 (CH19-U5 49 cm bs) to 29.27 (CH19-U1 65 cm bs) with a mean of 17.79. For the seasonally frozen ground samples, the C/N ratio range is between 13.77 (FI20-S-3P 92.5 cm bs) and 51.20 (FI20-S-3P 9.5 cm bs) with a mean of 29.78. C/N values most often show a decrease over depth (Fig. S1), but are similar across grazing intensities.

4.3 Stable carbon isotope ratio

Stable carbon isotope ratios ($\delta^{13}C$) values range from -30.61 ‰ (CH19-B5 5.75 cm bs) to -23.49 ‰ (CH19-U5 49 cm bs) with a mean of -27.43 ‰ for the permafrost-affected samples. For seasonally frozen ground samples, the range is -28.93 ‰ (FI20-S-5P 127.5 cm bs) to -26.44 ‰ (FI20-S-3M 38.5 cm bs) with a mean of -27.52 ‰. Values are generally similar over depth at each site, but different across sites (Fig. S1). At the permafrost sites, a general trend

to lighter $\delta^{13}C$ values can be observed with increasing grazing intensity, which is less clear for the seasonally frozen ground.

4.4 Absolute *n*-alkane concentration

The absolute lipid concentration of the *n*-alkanes in permafrost-affected samples range from 1.5 $\mu g/g_{TOC}$ (CH19-B3 71.5 cm bs) to 170.3 $\mu g/g_{TOC}$ (CH19-B1 124 cm bs). With a large share of samples having rather low concentrations, the mean value is 36.5 $\mu g/g_{TOC}$ with a median of 26.2 $\mu g/g_{TOC}$. In seasonally frozen ground samples, the *n*-alkane concentration varies between 1.7 $\mu g/g_{TOC}$ (FI20-S-5F 22.5 cm bs) and 117.8 $\mu g/g_{TOC}$ (FI22-W-5P-A 47.5 cm bs). The mean value is 22.2 $\mu g/g_{TOC}$, the median is 8.1 $\mu g/g_{TOC}$.

Concentrations follow no general pattern over depth across sites (Fig. S1), but are generally lower at sites occasionally grazed. Dung reference samples show values of 2.3 $\mu g/g_{TOC}$ (horse) and 14.3 $\mu g/g_{TOC}$ (reindeer).

4.5 Average chain length

Across permafrost-affected sites, $ACL_{23\text{-}33}$ of the *n*-alkanes ranges between 26.1 (CH19-B1 87.5 cm bs) and 28.6 (CH19-U5 93 cm bs) with a mean value of 27.65. For seasonally frozen ground, the $ACL_{23\text{-}33}$ range is 25.7 (sample FI-S-2M 18.5 cm bs) to 30.7 (FI22-W-3P 17.5 cm bs) with a mean of 28.3. The values for our reference dung samples are 28.5 for horse dung and 30.7 for reindeer dung (Fig. 2 & 3).

4.6 Carbon preference index

For permafrost-affected samples, the $CPI_{23\text{-}33}$ ranges from 3.8 (CH19-B1 26.25 cm bs) to 14.5 (CH19-U1 65 cm bs) and a mean value of 7.9. The median is 7.7.

The $CPI_{23\text{-}33}$ for seasonally frozen ground samples ranges from 5.0 (FI20-S-5M 11.5 cm bs) to 40.5 (FI22-W-3P 17.5 cm bs) with a mean value of 15.9 and a median of 11.1 in $CPI_{23\text{-}33}$. There is no general trend visible (Fig. S1). CPI for the horse dung reference sample is 23.3, and for reindeer dung 62.2 (Fig. 2).

For one sample from seasonally frozen ground (FI20-S-2M 18.5 cm bs), we were not able to calculate the CPI_{23-33} due to the absence of *n*-alkanes with even carbon lengths between 24 and 32. The CPI_{23-33} data indicate a slight trend to higher values with increasing grazing intensity at the permafrost and less clear also at the seasonally frozen ground sites (Fig. 2).

4.7 Higher-plant alcohol index

HPA of permafrost-affected samples ranges from 0.37 (CH19-B1 87.5 cm bs) to 0.90 (CH19-B5 106 cm bs) with a mean of 0.69 and a median of 0.70. For seasonally frozen ground samples, HPA ranges between 0.05 (FI20-S-5P 10 cm bs) and 0.88 (FI20-S-2M 18.5 cm bs) with a mean value of 0.34 and a median of 0.29. No general trend is visible over depth (Fig. S1). Values are generally higher for intensively grazed sites (Fig. 2). The dung reference samples show values of 0.44 (horse) and 0.23 (reindeer). For one seasonally frozen ground sample (FI20-S-3P 9.5 cm bs), we could not calculate the HPA index due to measurement issues.

4.8 Statistical results

We found no distinct differences between permafrost sites (Siberia) and seasonally frozen sites (Finland) that are consistent throughout all parameters. However, for individual parameters, and especially the HPA index, some differences were evident from our data. We found positive correlation for C/N ratio and CPI_{23-33} ($R = 0.60$) as well as for ACL and $\delta^{13}C$ ($R = 0.37$). At the same time, we found a strong negative correlation for HPA and TOC ($R = -0.57$).

We tested for statistically significant differences in biomarker parameters, comparing the permafrost-affected samples and the samples from seasonally frozen ground. We found a statistically significant difference for the HPA index between all samples from the permafrost environment (Siberia) and the seasonally frozen ground study area (Finland) (*p*-value < 0.001). For CPI_{23-33} we found a significant difference comparing the same set of samples (*p*-

value < 0.001). For ACL_{23-33} and absolute *n*-alkane concentration, the differences were not significant (*p*-value > 0.05).

However, when comparing HPA and CPI_{23-33} between grazing intensities, the differences were not significant.

To identify random effects in our dataset, especially spatial variation of the soil composition, and to identify if grazing intensity plays a role in parameter changes across our data, we run mixed effects models that showed positive interception values for HPA from permafrost sites in general, and for seasonally frozen sites with high grazing intensity. However, for seasonally frozen ground, this observation was not consistent, even though only negative values were returned for all seasonally frozen ground sites with a grazing intensity lower than pastures. Repeating this procedure for CPI_{23-33} produced clearly negative values for permafrost sites, and a range of values between -2.00 and 4.50 for seasonally frozen ground sites with no particular trend along grazing intensities or across soil types. The same holds for ACL_{23-33}, where the range for seasonally frozen ground sites is -0.78 and 1.04.

5 Discussion

5.1 Effects of grazing intensity on biomarker signals

Since animal activity influences OM storage and likely also OM decomposition in permafrost-affected areas (Windirsch *et al.* 2022a), we expected to find differences in the stored OM between different animal grazing intensities. We summarised our findings from *n*-alkane and *n*-alcohol analysis with a visualization figure (Fig. 4), and limited the comparison to samples taken from the top 38 cm of soil, as this was the minimum depth of encountered active layers in permafrost areas (Windirsch *et al.* 2022a), and the rather recent introduction of large herbivores (23 years in Siberia, 50 years in Finland)affects soil properties from the surface downwards.

453 The increasing HPA values in surface samples demonstrated the effects of grazing intensity,
454 with higher values associated with more intensive grazing. The single HPA value available for
455 occasional grazing aligns between exclosure and pasture samples. For the seasonally frozen
456 soils, this trend is not as strong due to one higher HPA value at exclosures and one lower
457 value at the pasture sites. Nevertheless, the presence of three of the four highest HPA values
458 at pasture sites suggests that the OM stored at sites of higher grazing intensity often shows a
459 lower OM transformation and thus degradation level. This supports our hypothesis that animal
460 grazing can have a preserving effect on soil OM. The reason for this could be that intense
461 grazing reduces the soil cover of sturdy and snow-catching shrub vegetation, in favour of
462 graminoid-dominated vegetation types, leading to faster and stronger soil cooling when air
463 temperatures drop in autumn/winter causing reduced OM degradation in surface soils. In the
464 permafrost-affected environment, this also appears to have an impact on the total carbon
465 storage with highest OC contents found at sites of occasional grazing and pasture. We did not
466 see this for the seasonally frozen ground sites, with partly very high TOC values at
467 occasionally grazed and pasture sites due to the fact that they are peat deposits, which makes
468 them hardly comparable to the mineral soil sites found in exclosure samples in terms of TOC
469 content. Further, soil compression from animal trampling often plays an important role on peat
470 soils, leading to higher bulk densities and therefore OC stocks. However, this was not the case
471 in this specific study area, as bulk density was not increasing under animal trampling on these
472 study sites but in fact decreasing, as reported in Windirsch *et al.* (2023c). The CPI_{23-33} data
473 also show a slight trend towards higher values (less decomposed) with increasing grazing
474 intensity especially at the permafrost sites. For the seasonally frozen ground samples, the
475 data show a lot more variation which is most likely related to a higher heterogeneity of the
476 source OM (including peat samples) in this area (Jongejans *et al.* 2020). Previous studies
477 showed that increased degradation within soils can also lead to an increase of the $\delta^{13}C$ values
478 of the remaining organic biomass due to the fact that isotopically lighter OM is preferentially
479 degraded by microorganisms (Barker and Fritz 1981). Thus, $\delta^{13}C$ values are often used as an
480 additional parameter for OM degradation (Bonanomi *et al.* 2013, Biester *et al.* 2014, Strauss

et al. 2015). Here, the $\delta^{13}C$ values of the soil OM show a trend towards lighter values and therefore less degraded OM with increased grazing intensity for both areas. This would additionally support our hypothesis that higher grazing intensity leads to lower OM decomposition in the soils due to the increased exposure of the soils to the winter cold. As mentioned before, $\delta^{13}C$ values can also be influenced by the $\delta^{13}C$ signal of the source OM. However, in this case a change from shrub-dominated environment ($\delta^{13}C$ values around -28 ‰ (Pattison and Welker 2014)) at lower grazing intensity to a graminoid-dominated environment ($\delta^{13}C$ values around -26 ‰ (Pattison and Welker 2014)) at higher grazing intensity should lead to an opposite trend indicating that the $\delta^{13}C$ signal of the source OM is not the determining factor of the bulk $\delta^{13}C$ signal of the deposited OM at least for the permafrost sites. This might be different for the seasonally frozen ground sites where some of the samples at grazing intensities 3 and 5 are organic-rich peat samples. Peats in this area are for instance dominated by *Sphagnum* species with $\delta^{13}C$ signals around -29 ‰ (Preis *et al.* 2018) and might be responsible for the higher variability of bulk $\delta^{13}C$ signals in the Finland dataset. While the ACL values exhibit clear differences between different grazing intensities, which is also in support of different vegetation compositions, we cannot state if these differences originate from any recent vegetation shifts triggered by grazing activity or from the original soil OM itself.

While soil cooling via animal activity and hence reduced OM decomposition are a possible explanation for increased OM stability at pastures, the stable and undisturbed growth of ground-covering and therefore insulating species such as *Cladonia rangiferina* (L.) Weber ex F.H.Wigg. observed at the Finland site (Windirsch *et al.* 2023c) might be a plausible explanation for the low decomposition state of the sample with an exceptionally high (> 0.5) HPA value found at an exclosure site (Porada *et al.* 2016). Such light-coloured lichen lead to a high area albedo while at the same time form an insulating air layer on top of the ground. Although a dense cover of *C. rangiferina* can therefore act as an insulation layer for the soil against low winter temperatures, it also insulates against summer heat to some degree, in

508 contrast to graminoid vegetation. Therefore, in artificially undisturbed areas where such a layer
509 can form, the summer shadowing effects lead to generally lower soil temperature amplitudes
510 which might partially compensate for the total absence of the positive large-mammal herbivore
511 effect on the OM preservation. However, this only works in areas where herbivores can be
512 excluded (e.g. by fences) and also where environmental characteristics are enabling such a
513 light-coloured but not trampling-resistant vegetation type to grow. At the occasionally grazed
514 sites, animal impact is too strong for such an insulating lichen layer to form, but too weak for
515 animal-induced vegetation shifts towards graminoid-dominated vegetation and effective soil
516 cooling by snow trampling and mentioned vegetation change leading to intermediate OM
517 degradation.
518
519 **5.2 Effects of ground thermal regime on soil OM degradation**
520 Depositional areas were clearly distinguished by the CPI, ACL and HPA index data into
521 permafrost-affected (Siberia) and seasonally frozen ground (Finland). While the active layer
522 and deeper permafrost deposits show variations within a similar range, the seasonally frozen
523 ground samples show a distinct offset. The ACL and CPI for the Finland sites are notably
524 higher, which is due to differences of the vegetational composition of both sites. As shown
525 before with the dung samples, the permafrost sites are dominated by *Calamagrostis* ssp.
526 Adans. which shows a lower ACL (28) (Berke *et al.* 2019) than *Deschampsia cespitosa* (L.)
527 P.Beauv. (ACL 30.3) (Gamarra and Kahmen 2015) mixed with *Sphagnum* Linné (ACL 25.9)
528 (Huang *et al.* 2012) at the Finland sites. Additionally, the seasonal frozen ground also contains
529 a high number of peat samples (21 out of 32) supporting the assumption of different OM
530 compositions. When examining the HPA index, a significant difference (with a p-value of 1.08^{-7})
531 between these deposits or rather study areas is found. The samples from the examined
532 permafrost and active layer have a median HPA of 0.70, while the seasonally frozen ground
533 has a significantly lower median HPA of 0.27. Generally, HPA values are lower than 0.50 in
534 the seasonally frozen ground samples, while samples from the permafrost study area are
535 higher than 0.50 (Fig. 3). Thus, the HPA data, generally, indicate a higher level of OM

preservation for the permafrost deposits, which can be related to the reduced annual time of OM degradation which is limited to the period when the soil is not frozen (Schuur *et al.* 2008, Strauss *et al.* 2015, Walz *et al.* 2017).

Whether direct digestion of the OM by the local herbivore community may contribute to the overall degradation pattern is difficult to say, since the proportion of the digested OM relative to the total OM is unknown. However, such a contribution might be indicated when comparing the HPA values of the horse (HPA of 0.44) and reindeer dung (HPA of 0.23), showing a higher degree of degradation of the OM at the Finland site in the reindeer sample. When comparing the reindeer dung ACL values with those from literature for graminoid species (Gamarra and Kahmen 2015), the dung signal and the mean signal of the most abundant graminoid species at the study site, *Deschampsia cespitosa* (L.) P.Beauv., are quite similar. For the horse dung (Siberia), which is expected to contain mainly locally predominating *Calamagrostis* Adans. material, the ACL value is in good agreement to the ACL value reported for another species of the *Calamagrostis* genus (Berke *et al.* 2019), although slightly shifted towards shorter chains. Thus, the horse dung from the Siberian study area likely contains mainly *Calamagrostis* material with a minor content of other plant material. However, the dung ACL values differ from the examined soils sampled at pasture sites, suggesting that dung is not the main input for these soils but a wider mix of plant material is present in the ground. Although only one dung sample has been investigated in each study area, and therefore cannot be considered representative, the measured dung samples seem to reflect the source OM signal rather than deposited OM. For the permafrost sites, where the active layer shows a slightly lower HPA value than the underlying permafrost, we can therefore assume that in the active layer we have a mixed signal between the original substrate, preserved below in the permafrost, and the recent vegetation, either directly or via animal faeces. This mixing could also explain the low HPA values in pasture samples from seasonally frozen ground, where the low reindeer dung HPA, either representing the current vegetation or the animal influence, could lower the overall HPA value of a sample.

564 Overall, the applied biomarker parameters are valuable to show significant differences in
565 organic source material (ACL in dung samples) and level of OM degradation (HPA) between
566 the permafrost and seasonal frozen ground site and to clearly distinguish both sites. In terms
567 of the different grazing intensities at each location, the parameters work better for the
568 permafrost site, while trends are less distinct for the seasonal-frozen ground site. This is also
569 where the authors would see the method's potential future use in grazing impact assessment.
570 A reason for this is most likely that, despite the ongoing OM degradation, the OM is still in an
571 overall geologically immature stage at both sites and that at this stage variations in the OM
572 source material can still have an influence on the biomarker parameters (CPI). Such an impact
573 is particularly evident at the seasonal-frozen ground site, where the TOC values are highly
574 variable and OM types (mineral soils vs. peat deposits) can be very different. Evaluating the
575 success of this pilot study - utilising lipid biomarkers to identify animal impacts on soil
576 characteristics - we can confirm that differences in OM decomposition, which we linked to
577 animal activity, can be read from the biomarker results. We therefore deem this method
578 suitable for similar research problems, taking additional precautions like a larger set of
579 samples, and a more balanced sampling strategy.
580
581 **5.3 Impact of herbivory on permafrost OM storage**
582 The bulk $\delta^{13}C$, $CPI_{23\text{-}33}$ and HPA values suggest that intensive grazing (pasture) land use
583 tends to lead to less decomposed OM (Fig. 2) in the Arctic regions. However, partly variable
584 data at the permafrost but particularly at the seasonally frozen ground sites indicate that also
585 other factors such as the composition of the organic source material can have an impact on
586 the assessment of the OM decomposition level. Overall, the data suggest that degradation of
587 functionalized OM might generally be lower in permafrost-affected soils. This leads to the
588 conclusion that the thermal conditions in the soil have an impact on the biomarker composition
589 via reduced OM degradation. The extent to which the soil thermal conditions are influenced
590 by animal activity via snow trampling and pasture-related vegetation changes is difficult to
591 assess on the basis of the current pilot study dataset.

592 The differences between grazing intensities (Fig. 4) observed in this pilot study are mainly
593 trends that are not statistically well supported due to the data variability. It also has to be kept
594 in mind that the observed differences are the result of a relatively short time period between
595 the beginning of grazing and sampling (23 years for permafrost-affected sites, 50 years for
596 seasonally frozen ground sites) and that in addition to time the effects also depend on the
597 animal densities to be observed across a whole area, which both also contributes to the data
598 variability. Also, differences between grazing intensities in seasonally frozen ground sites
599 could be due to random effects caused by spatial variability such as heterogeneity of soil
600 material, hydrology or relief position. While there are differences observed, and these
601 differences approximately match our expectations of less degraded material under high
602 grazing impact, our mixed effects modelling (section 4.8) revealed that variability between
603 sites even within grazing intensities is high, making spatial heterogeneity an important factor
604 to consider. On the other hand, the model confirmed that HPA and CPI_{23-33}, which we used as
605 degradation proxies, indicate a generally less decomposed state of soil OM for the permafrost-
606 affected sites, reporting highest interception values for the permafrost sites, clearly above the
607 interception baseline of the complete dataset.
608 At our study sites, the herbivore densities are unnaturally increased, and still grazing-related
609 effects are rather small. Thus, actively utilising herbivory to reduce OM decomposition might
610 therefore only be feasible on a very local scale where animals can be herded and controlled
611 over longer periods of time of at least 20 to 50 years to see first effects of grazing activity.
612 Further studies on this topic are advised, including detailed measurements of each site's
613 preconditions and a higher spatial resolution of sampling points as well as replicate sampling
614 to account for confounding factors.
615

616 **6 Conclusion**

617 Building upon the hypothesis that large herbivore activity contributes to colder ground
618 temperatures by keeping the soil vegetation low and thereby slowing down OM decomposition,
619 we have found indications that both permafrost-affected and to a smaller extend also

seasonally frozen Arctic ground tend to exhibit better-preserved soil OM under high grazing intensity. Based on our lipid biomarker screening data we also observed, in addition to the grazing effect, an overall lower degradation level of the permafrost OM compared to OM in the seasonally frozen ground. The grazing effect on the OM preservation was evident in data trends but was not statistically well confirmable. This was most likely due to high spatial variability of the examined soil material (including different source OM) and little expressed changes in the biomarker signals.

Nevertheless, we see indications that intensive herbivory tends to have a positive impact on soil carbon storage in permafrost, while in seasonally frozen ground an effect is not clearly visible or more strongly masked by random effects such as soil material differences and overall spatial heterogeneity (i.e. micro-topography, vegetation, hydrology etc.). At the same time, we also found no negative impact of herbivory on soil carbon storage in seasonally frozen ground. These results need to be evaluated in future studies with a more dense and well balanced sampling approach. We still suggest that the implementation of intensive herbivory practices may offer localised opportunities for mitigating OM decomposition and subsequently reducing carbon emissions originating from permafrost and should be further examined in climate change strategy development.

7 Acknowledgements

The authors gratefully acknowledge Anke Kaminski and Cornelia Karger from the GFZ Organic Geochemistry laboratory facilities for their invaluable guidance and assistance in lipid biomarker sample preparation and measurement. They would also like to express their appreciation to the AWI's Permafrost Carbon and Nitrogen Lab, especially Justin Lindemann for his expert assistance with sample preparation. Furthermore, the authors extend their gratitude to J. Otto Habeck (Universität Hamburg) for his valuable contributions to the design of this study.

8 Competing interests

The authors declare no conflict of interests, neither commercial nor financially nor ethical.

9 Author contribution

TW and JS designed this pilot study. KM, LJ and JS provided expertise in biomarker analysis and interpretation. TW, GG, JW and JS put the data into local environment context. All authors contributed to writing and editing the manuscript.

10 Funding

This research was carried out as part of the PeCHEc (Permafrost Carbon Stabilisation by Recreating a Herbivore-Driven Ecosystem) project. This project was funded by the Potsdam Graduate School, supported by the AWI Permafrost Research section and the Geo.X research network (SO_087_GeoX).

Field campaigns were financed by the CACOON (Changing Arctic Carbon Cycle in the Coastal Ocean Near-Shore) project (#03F0806A (German Federal Ministry of Education and Research)) and the AWI and the Permafrost Research section baseline and expedition funding.

11 Data availability

The biomarker measurement data as well as all other data used in this manuscript are available from the PANGAEA repository (Windirsch *et al.* 2021b, Windirsch *et al.* 2022b; c, Windirsch *et al.* 2023a; b).

12 References

Barker, J. F. & Fritz, P. 1981. *Carbon isotope fractionation during microbial methane oxidation*. Nature 293 (5830): 289-291, doi:10.1038/293289a0.

Beer, C., Zimov, N., Olofsson, J., Porada, P. & Zimov, S. 2020. *Protection of Permafrost Soils from Thawing by Increasing Herbivore Density*. Scientific Reports 10 (1): 4170, doi:10.1038/s41598-020-60938-y.

Berke, M. A., Cartagena Sierra, A., Bush, R., Cheah, D. & O'Connor, K. 2019. *Controls on leaf wax fractionation and δ2H values in tundra vascular plants from western Greenland*. Geochimica et Cosmochimica Acta 244: 565-583, doi:10.1016/j.gca.2018.10.020.

679 Biester, H., Knorr, K. H., Schellekens, J., Basler, A. & Hermanns, Y. M. 2014. *Comparison of*
680 *different methods to determine the degree of peat decomposition in peat bogs*.
681 Biogeosciences 11 (10): 2691-2707, doi:10.5194/bg-11-2691-2014.
682 Blok, D., Heijmans, M. M. P. D., Schaepman-Strub, G., Kononov, A. V., Maximov, T. C. &
683 Berendse, F. 2010. *Shrub expansion may reduce summer permafrost thaw in Siberian*
684 *tundra*. Global Change Biology 16 (4): 1296-1305, doi:10.1111/j.1365-
685 2486.2009.02110.x.
686 Bonanomi, G., Incerti, G., Giannino, F., Mingo, A., Lanzotti, V. & Mazzoleni, S. 2013. *Litter*
687 *quality assessed by solid state 13C NMR spectroscopy predicts decay rate better than*
688 *C/N and Lignin/N ratios*. Soil Biology and Biochemistry 56: 40-48,
689 doi:10.1016/j.soilbio.2012.03.003.
690 Bowen, J. C., Ward, C. P., Kling, G. W. & Cory, R. M. 2020. *Arctic Amplification of Global*
691 *Warming Strengthened by Sunlight Oxidation of Permafrost Carbon to CO2*.
692 Geophysical Research Letters 47 (12): e2020GL087085,
693 doi:10.1029/2020GL087085.
694 Bradley, H. & Stein, S. 2022. *Climate opportunism and values of change on the Arctic*
695 *agricultural frontier*. Economic Anthropology 9 (2): 207-222, doi:10.1002/sea2.12251.
696 Bray, E. E. & Evans, E. D. 1961. *Distribution of n-paraffins as a clue to recognition of source*
697 *beds*. Geochimica et Cosmochimica Acta 22 (1): 2-15, doi:10.1016/0016-
698 7037(61)90069-2.
699 Coplen, T. B., Brand, W. A., Gehre, M., Gröning, M., Meijer, H. A. J., Toman, B. & Verkouteren,
700 R. M. 2006. *New Guidelines for δ13C Measurements*. Analytical Chemistry 78 (7):
701 2439-2441, doi:10.1021/ac052027c.
702 Corradi, C., Kolle, O., Walter, K., Zimov, S. A. & Schulze, E.-D. 2005. *Carbon dioxide and*
703 *methane exchange of a north-east Siberian tussock tundra*. Global Change Biology 11
704 (11): 1910-1925, doi:10.1111/j.1365-2486.2005.01023.x.
705 Finnish Meteorological Institute. 2021. *Observation data (monthly observations) for station*
706 *102047 Inari Kaamanen, 2008-2020*. accessed 17.09.2021.
707 https://en.ilmatieteenlaitos.fi/download-observations.
708 Forbes, B. C., Ebersole, J. J. & Strandberg, B. 2001. *Anthropogenic Disturbance and Patch*
709 *Dynamics in Circumpolar Arctic Ecosystems*. Conservation Biology 15 (4): 954-969,
710 doi:10.1046/j.1523-1739.2001.015004954.x.
711 Fuchs, M., Bolshiyanov, D., Grigoriev, M. N., Morgenstern, A., Pestryakova, L., Tsibizov, L. &
712 Dill, A. 2021. *Russian-German Cooperation: Expeditions to Siberia in 2019*. Alfred
713 Wegener Institute for Polar and Marine Research, Bremerhaven, available at
714 https://epic.awi.de/id/eprint/53575/.
715 Gamarra, B. & Kahmen, A. 2015. *Concentrations and δ2H values of cuticular n-alkanes vary*
716 *significantly among plant organs, species and habitats in grasses from an alpine and*
717 *a temperate European grassland*. Oecologia 178 (4): 981-998, doi:10.1007/s00442-
718 015-3278-6.
719 Genet, H., McGuire, A. D., Barrett, K., Breen, A., Euskirchen, E. S., Johnstone, J. F.,
720 Kasischke, E. S., Melvin, A. M., Bennett, A., Mack, M. C., Rupp, T. S., Schuur, E. A.
721 G., Turetsky, M. R. & Yuan, F. 2013. *Modeling the effects of fire severity and climate*
722 *warming on active layer thickness and soil carbon storage of black spruce forests*
723 *across the landscape in interior Alaska*. Environmental Research Letters 8 (4): 045016,
724 doi:10.1088/1748-9326/8/4/045016.
725 Glombitza, C., Mangelsdorf, K. & Horsfield, B. 2009. *Maturation related changes in the*
726 *distribution of ester bound fatty acids and alcohols in a coal series from the New*
727 *Zealand Coal Band covering diagenetic to catagenetic coalification levels*. Organic
728 geochemistry 40 (10): 1063-1073, doi:10.1016/j.orggeochem.2009.07.008.
729 Göckede, M., Kittler, F., Kwon, M. J., Burjack, I., Heimann, M., Kolle, O., Zimov, N. & Zimov,
730 S. 2017. *Shifted energy fluxes, increased Bowen ratios, and reduced thaw depths*
731 *linked with drainage-induced changes in permafrost ecosystem structure*. The
732 Cryosphere 11 (6): 2975-2996, doi:10.5194/tc-11-2975-2017.

Golubtsov, V. A., Vanteeva, Y. V., Voropai, N. N., Vasilenko, O. V., Cherkashina, A. A. & Zazovskaya, E. P. 2022. *Stable Carbon Isotopic Composition (δ13C) as a Proxy of Organic Matter Dynamics in Soils on the Western Shore of Lake Baikal*. Eurasian Soil Science 55 (12): 1700-1713, doi:10.1134/S1064229322700041.

Grellmann, D. 2002. *Plant responses to fertilization and exclusion of grazers on an arctic tundra heath*. Oikos 98 (2): 190-204, doi:10.1034/j.1600-0706.2002.980202.x.

Grosse, G., Harden, J., Turetsky, M., McGuire, A. D., Camill, P., Tarnocai, C., Frolking, S., Schuur, E. A. G., Jorgenson, T., Marchenko, S., Romanovsky, V., Wickland, K. P., French, N., Waldrop, M., Bourgeau-Chavez, L. & Striegl, R. G. 2011. *Vulnerability of high-latitude soil organic carbon in North America to disturbance*. Journal of Geophysical Research: Biogeosciences 116 (G4) doi:10.1029/2010JG001507.

Harden, J. W., Manies, K. L., Turetsky, M. R. & Neff, J. C. 2006. *Effects of wildfire and permafrost on soil organic matter and soil climate in interior Alaska*. Global Change Biology 12 (12): 2391-2403, doi:10.1111/j.1365-2486.2006.01255.x.

Huang, X., Xue, J., Zhang, J., Qin, Y., Meyers, P. A. & Wang, H. 2012. *Effect of different wetness conditions on Sphagnum lipid composition in the Erxianyan peatland, central China*. Organic geochemistry 44: 1-7, doi:10.1016/j.orggeochem.2011.12.005.

Hugelius, G., Loisel, J., Chadburn, S., Jackson, R. B., Jones, M., MacDonald, G., Marushchak, M., Olefeldt, D., Packalen, M., Siewert, M. B., Treat, C., Turetsky, M., Voigt, C. & Yu, Z. 2020. *Large stocks of peatland carbon and nitrogen are vulnerable to permafrost thaw*. PNAS 117 (34): 20438-20446, doi:10.1073/pnas.1916387117.

IPCC. 2021. *Climate Change 2021: The Physical Science Basis. Contribution of Working Group I to the Sixth Assessment Report of the Intergovernmental Panel on Climate Change*. IPCC, Cambridge University Press, available.

Jones, B. M., Grosse, G., Arp, C. D., Miller, E., Liu, L., Hayes, D. J. & Larsen, C. F. 2015. *Recent Arctic tundra fire initiates widespread thermokarst development*. Scientific Reports 5 (1): 15865, doi:10.1038/srep15865.

Jongejans, L. L., Strauss, J., Lenz, J., Peterse, F., Mangelsdorf, K., Fuchs, M. & Grosse, G. 2018. *Organic matter characteristics in yedoma and thermokarst deposits on Baldwin Peninsula, west Alaska*. Biogeosciences 15 (20): 6033-6048, doi:10.5194/bg-15-6033-2018.

Jongejans, L. L., Mangelsdorf, K., Schirrmeister, L., Grigoriev, M. N., Maksimov, G. M., Biskaborn, B. K., Grosse, G. & Strauss, J. 2020. *n-Alkane Characteristics of Thawed Permafrost Deposits Below a Thermokarst Lake on Bykovsky Peninsula, Northeastern Siberia*. Frontiers in Environmental Science 8 doi:10.3389/fenvs.2020.00118.

Jongejans, L. L., Liebner, S., Knoblauch, C., Mangelsdorf, K., Ulrich, M., Grosse, G., Tanski, G., Fedorov, A. N., Konstantinov, P. Y., Windirsch, T., Wiedmann, J. & Strauss, J. 2021. *Greenhouse gas production and lipid biomarker distribution in Yedoma and Alas thermokarst lake sediments in Eastern Siberia*. Global Change Biology 27 (12): 2822-2839, doi:10.1111/gcb.15566.

Kaplan, J. O., Krumhardt, K. M., Ellis, E. C., Ruddiman, W. F., Lemmen, C. & Goldewijk, K. K. 2010. *Holocene carbon emissions as a result of anthropogenic land cover change*. The Holocene 21 (5): 775-791, doi:10.1177/0959683610386983.

Kristensen, J. A., Svenning, J.-C., Georgiou, K. & Malhi, Y. 2022. *Can large herbivores enhance ecosystem carbon persistence?* Trends in Ecology & Evolution 37 (2): 117-128, doi:10.1016/j.tree.2021.09.006.

Lal, R. 2022. Biophysical Controls That Make Erosion-Transported Soil Carbon a Source of Greenhouse Gases. *Applied Sciences* 12, 16, 10.3390/app12168372.

Macias-Fauria, M., Jepson, P., Zimov, N. & Malhi, Y. 2020. *Pleistocene Arctic megafaunal ecological engineering as a natural climate solution?* Philosophical Transactions of the Royal Society B: Biological Sciences 375 (1794): 20190122, doi:10.1098/rstb.2019.0122.

Maliniemi, T., Kapfer, J., Saccone, P., Skog, A. & Virtanen, R. 2018. *Long-term vegetation changes of treeless heath communities in northern Fennoscandia: Links to climate*

change trends and reindeer grazing. Journal of Vegetation Science 29 (3): 469-479, doi:10.1111/jvs.12630.

Marzi, R., Torkelson, B. E. & Olson, R. K. 1993. *A revised carbon preference index*. Organic geochemistry 20 (8): 1303-1306, doi:10.1016/0146-6380(93)90016-5.

Mekonnen, Z. A., Riley, W. J., Berner, L. T., Bouskill, N. J., Torn, M. S., Iwahana, G., Breen, A. L., Myers-Smith, I. H., Criado, M. G., Liu, Y., Euskirchen, E. S., Goetz, S. J., Mack, M. C. & Grant, R. F. 2021. *Arctic tundra shrubification: a review of mechanisms and impacts on ecosystem carbon balance*. Environmental Research Letters 16 (5): 053001, doi:10.1088/1748-9326/abf28b.

Monhonval, A., Mauclet, E., Pereira, B., Vandeuren, A., Strauss, J., Grosse, G., Schirrmeister, L., Fuchs, M., Kuhry, P. & Opfergelt, S. 2021. *Mineral Element Stocks in the Yedoma Domain: A Novel Method Applied to Ice-Rich Permafrost Regions*. Frontiers in Earth Science 9 doi:10.3389/feart.2021.703304.

Oksanen, L. & Virtanen, R. 1995. Topographic, altitudinal and regional patterns in continental and suboceanic heath vegetation of northern Fennoscandia. In: *Acta Botanica Fennica,* Finnish Zoological and Botanical Publishing Board, Helsinki, pp. 1-80

Olofsson, J. & Post, E. 2018. *Effects of large herbivores on tundra vegetation in a changing climate, and implications for rewilding*. Philosophical Transactions of the Royal Society B: Biological Sciences 373 (1761): 20170437, doi:10.1098/rstb.2017.0437.

Palmtag, J., Hugelius, G., Lashchinskiy, N., Tamstorf, M. P., Richter, A., Elberling, B. & Kuhry, P. 2015. *Storage, Landscape Distribution, and Burial History of Soil Organic Matter in Contrasting Areas of Continuous Permafrost*. Arctic, Antarctic, and Alpine Research 47 (1): 71-88, doi:10.1657/AAAR0014-027.

Paoli, A., Weladji, R. B., Holand, Ø. & Kumpula, J. 2018. *Winter and spring climatic conditions influence timing and synchrony of calving in reindeer*. PLOS ONE 13 (4): e0195603, doi:10.1371/journal.pone.0195603.

Park, H., Fedorov, A. N., Zheleznyak, M. N., Konstantinov, P. Y. & Walsh, J. E. 2015. *Effect of snow cover on pan-Arctic permafrost thermal regimes*. Climate Dynamics 44 (9): 2873-2895, doi:10.1007/s00382-014-2356-5.

Pattison, R. R. & Welker, J. M. 2014. *Differential ecophysiological response of deciduous shrubs and a graminoid to long-term experimental snow reductions and additions in moist acidic tundra, Northern Alaska*. Oecologia 174 (2): 339-350, doi:10.1007/s00442-013-2777-6.

Peplau, T., Schroeder, J., Gregorich, E. & Poeplau, C. 2022. *Subarctic soil carbon losses after deforestation for agriculture depend on permafrost abundance*. Global Change Biology 28 (17): 5227-5242, doi:10.1111/gcb.16307.

Porada, P., Ekici, A. & Beer, C. 2016. *Effects of bryophyte and lichen cover on permafrost soil temperature at large scale*. The Cryosphere 10 (5): 2291-2315, doi:10.5194/tc-10-2291-2016.

Poynter, J. 1989. *Molecular stratigraphy: The recognition of palea-climatic signals in organic geochemical data.* School of Chemistry, University of Bristol, Bristol.

Poynter, J. & Eglinton, G. 1990. *14. Molecular composition of three sediments from hole 717c: The Bengal fan*. In: Cochran J.R., Stow, D. A. V., et al. (ed.), *The Ocean Drilling Program, Scientific Results*.

Preis, Y. I., Simonova, G. V., Voropay, N. N. & Dyukarev, E. A. 2018. *Estimation of the influence of hydrothermal conditions on the carbon isotope composition in Sphagnum mosses of bogs of Western Siberia*. IOP Conference Series: Earth and Environmental Science 211 (1): 012031, doi:10.1088/1755-1315/211/1/012031.

Previdi, M., Smith, K. L. & Polvani, L. M. 2021. *Arctic amplification of climate change: a review of underlying mechanisms*. Environmental Research Letters 16 (9): 093003, doi:10.1088/1748-9326/ac1c29.

Radke, M., Willsch, H. & Welte, D. H. 1980. *Preparative hydrocarbon group type determination by automated medium pressure liquid chromatography*. Analytical Chemistry 52 (3): 406-411, doi:10.1021/ac50053a009.

Ramesh, T., Bolan, N. S., Kirkham, M. B., Wijesekara, H., Kanchikerimath, M., Srinivasa Rao, C., Sandeep, S., Rinklebe, J., Ok, Y. S., Choudhury, B. U., Wang, H., Tang, C., Wang, X., Song, Z. & Freeman Ii, O. W. 2019. Chapter One - Soil organic carbon dynamics: Impact of land use changes and management practices: A review. In: Sparks D.L. (ed.), *Advances in Agronomy,* Academic Press, pp. 1-107 doi:10.1016/bs.agron.2019.02.001.

R Core Team. 2021. *R: A language and environment for statistical computing*, *v4.1.1*. R Foundation for Statistical Computing, Vienna, Austria. https://www.R-project.org/.

Rutkowski, C., Lenz, J., Lang, A., Wolter, J., Mothes, S., Reemtsma, T., Grosse, G., Ulrich, M., Fuchs, M., Schirrmeister, L., Fedorov, A., Grigoriev, M., Lantuit, H. & Strauss, J. 2021. *Mercury in Sediment Core Samples From Deep Siberian Ice-Rich Permafrost*. Frontiers in Earth Science 9 doi:10.3389/feart.2021.718153.

Schuster, P. F., Schaefer, K. M., Aiken, G. R., Antweiler, R. C., Dewild, J. F., Gryziec, J. D., Gusmeroli, A., Hugelius, G., Jafarov, E., Krabbenhoft, D. P., Liu, L., Herman-Mercer, N., Mu, C., Roth, D. A., Schaefer, T., Striegl, R. G., Wickland, K. P. & Zhang, T. 2018. *Permafrost Stores a Globally Significant Amount of Mercury*. Geophysical Research Letters 45 (3): 1463-1471, doi:10.1002/2017GL075571.

Schuur, E. A. G., McGuire, A. D., Schädel, C., Grosse, G., Harden, J. W., Hayes, D. J., Hugelius, G., Koven, C. D., Kuhry, P., Lawrence, D. M., Natali, S. M., Olefeldt, D., Romanovsky, V. E., Schaefer, K., Turetsky, M. R., Treat, C. C. & Vonk, J. E. 2015. *Climate change and the permafrost carbon feedback*. Nature 520: 171, doi:10.1038/nature14338.

Schuur, E. A. G., Bockheim, J., Canadell, J. G., Euskirchen, E., Field, C. B., Goryachkin, S. V., Hagemann, S., Kuhry, P., Lafleur, P. M., Lee, H., Mazhitova, G., Nelson, F. E., Rinke, A., Romanovsky, V. E., Shiklomanov, N., Tarnocai, C., Venevsky, S., Vogel, J. G. & Zimov, S. A. 2008. *Vulnerability of Permafrost Carbon to Climate Change: Implications for the Global Carbon Cycle*. BioScience 58 (8): 701-714, doi:10.1641/B580807.

Schuur, E. A. G., Abbott, B. W., Commane, R., Ernakovich, J., Euskirchen, E., Hugelius, G., Grosse, G., Jones, M., Koven, C., Leshyk, V., Lawrence, D., Loranty, M. M., Mauritz, M., Olefeldt, D., Natali, S., Rodenhizer, H., Salmon, V., Schädel, C., Strauss, J., Treat, C. & Turetsky, M. 2022. *Permafrost and Climate Change: Carbon Cycle Feedbacks From the Warming Arctic*. Annual Review of Environment and Resources 47 (1): 343-371, doi:10.1146/annurev-environ-012220-011847.

Stimmler, P., Goeckede, M., Elberling, B., Natali, S., Kuhry, P., Perron, N., Lacroix, F., Hugelius, G., Sonnentag, O., Strauss, J., Minions, C., Sommer, M. & Schaller, J. 2023. *Pan-Arctic soil element bioavailability estimations*. Earth Syst. Sci. Data 15 (3): 1059-1075, doi:10.5194/essd-15-1059-2023.

Strauss, J., Schirrmeister, L., Mangelsdorf, K., Eichhorn, L., Wetterich, S. & Herzschuh, U. 2015. *Organic-matter quality of deep permafrost carbon – a study from Arctic Siberia*. Biogeosciences 12 (10.5194/bg-12-2227-2015): 2227-2245, doi:10.5194/bg-12-2227-2015.

Strauss, J., Abbott, B. W., Hugelius, G., Schuur, E., Treat, C., Fuchs, M., Schädel, C., Ulrich, M., Turetsky, M. & Keuschnig, M. 2021. 9. Permafrost. In: *Recarbonizing global soils–A technical manual of recommended management practices: Volume 2–Hot spots and bright spots of soil organic carbon,* p. 130

Strauss, J., Biasi, C., Sanders, T., Abbott, B. W., von Deimling, T. S., Voigt, C., Winkel, M., Marushchak, M. E., Kou, D., Fuchs, M., Horn, M. A., Jongejans, L. L., Liebner, S., Nitzbon, J., Schirrmeister, L., Walter Anthony, K., Yang, Y., Zubrzycki, S., Laboor, S., Treat, C. & Grosse, G. 2022. *A globally relevant stock of soil nitrogen in the Yedoma permafrost domain*. Nature Communications 13 (1): 6074, doi:10.1038/s41467-022-33794-9.

Stroeven, A. P., Hättestrand, C., Kleman, J., Heyman, J., Fabel, D., Fredin, O., Goodfellow, B. W., Harbor, J. M., Jansen, J. D., Olsen, L., Caffee, M. W., Fink, D., Lundqvist, J.,

Rosqvist, G. C., Strömberg, B. & Jansson, K. N. 2016. *Deglaciation of Fennoscandia*. Quaternary Science Reviews 147: 91-121, doi:10.1016/j.quascirev.2015.09.016.

Turetsky, M. R., Abbott, B. W., Jones, M. C., Walter Anthony, K., Olefeldt, D., Schuur, E. A. G., Koven, C., McGuire, A. D., Grosse, G., Kuhry, P., Hugelius, G., Lawrence, D. M., Gibson, C. & Sannel, A. B. K. 2019. *Permafrost collapse is accelerating carbon release*. Nature doi:10.1038/d41586-019-01313-4.

van Groenigen, K. J., Osenberg, C. W. & Hungate, B. A. 2011. *Increased soil emissions of potent greenhouse gases under increased atmospheric CO2*. Nature 475 (7355): 214-216, doi:10.1038/nature10176.

Veremeeva, A., Nitze, I., Günther, F., Grosse, G. & Rivkina, E. 2021. *Geomorphological and Climatic Drivers of Thermokarst Lake Area Increase Trend (1999–2018) in the Kolyma Lowland Yedoma Region, North-Eastern Siberia*. Remote Sensing 13 (2): 178, doi:10.3390/rs13020178.

Walz, J., Knoblauch, C., Böhme, L. & Pfeiffer, E.-M. 2017. *Regulation of soil organic matter decomposition in permafrost-affected Siberian tundra soils - Impact of oxygen availability, freezing and thawing, temperature, and labile organic matter*. Soil Biology and Biochemistry 110: 34-43, doi:10.1016/j.soilbio.2017.03.001.

Ward Jones, M., Habeck, J. O., Ulrich, M., Crate, S., Gannon, G., Schwoerer, T., Jones, B., Kanevskiy, M., Baral, P., Maharjan, A., Steiner, J., Spring, A., Price, M. J., Bysouth, D., Forbes, B. C., Verdonen, M., Kumpula, T., Strauss, J., Windirsch, T., Poeplau, C., Shur, Y., Gaglioti, B., Parlato, N., Tao, F., Turetsky, M., Grand, S., Unc, A. & Borchard, N. 2024. *Socioecological dynamics of diverse global permafrost-agroecosystems under environmental change*. Arctic, Antarctic, and Alpine Research 56 (1): 2356067, doi:10.1080/15230430.2024.2356067.

Windirsch, T., Fuchs, M., Grosse, G., Habeck, J. O., Ulrich, M. & Strauss, J. 2021a. Expedition to Kutuharju Field Research Station, Northern Finland, September 2020. In: Fuchs M., van Delden L., Lehmann N. & Windirsch T. (eds.), *Expeditions to Fennoscandia in 2020,* Berichte zur Polar- und Meeresforschung = Reports on polar and marine research, Alfred Wegener Institute for Polar and Marine Research, Bremerhaven, pp. 5-12 doi:10.48433/BzPM_0752_2021.

Windirsch, T., Mangelsdorf, K., Grosse, G., Wolter, J., Jongejans, L. L. & Strauss, J. 2023a. *n-Alkane characteristics of Arctic soils, comparing different large herbivore grazing intensities under permafrost and non-permafrost conditions*. PANGAEA. doi:10.1594/PANGAEA.963258.

Windirsch, T., Mangelsdorf, K., Grosse, G., Wolter, J., Jongejans, L. L. & Strauss, J. 2023b. *n-alcohol characteristics of Arctic soils, comparing different large herbivore grazing intensities under permafrost and non-permafrost conditions*. PANGAEA. doi:10.1594/PANGAEA.963259.

Windirsch, T., Grosse, G., Ulrich, M., Forbes, B. C., Göckede, M., Zimov, N., Macias-Fauria, M., Olofsson, J., Wolter, J. & Strauss, J. 2021b. *Large herbivores affecting terrestrial permafrost in northeastern Siberia: biogeochemical and sediment characteristics under different grazing intensities*. PANGAEA. doi:10.1594/PANGAEA.933446.

Windirsch, T., Grosse, G., Ulrich, M., Forbes, B. C., Göckede, M., Wolter, J., Macias-Fauria, M., Olofsson, J., Zimov, N. & Strauss, J. 2022a. *Large herbivores on permafrost— a pilot study of grazing impacts on permafrost soil carbon storage in northeastern Siberia*. Frontiers in Environmental Science 10 doi:10.3389/fenvs.2022.893478.

Windirsch, T., Forbes, B. C., Grosse, G., Wolter, J., Treat, C. C., Ulrich, M., Stark, S., Fuchs, M., Olofsson, J., Macias-Fauria, M., Kumpula, T. & Strauss, J. 2022b. *Peat and sediment characteristics from different Reindeer grazing intensities in Northern Finland*. PANGAEA. doi:10.1594/PANGAEA.941930.

Windirsch, T., Forbes, B. C., Grosse, G., Wolter, J., Treat, C. C., Ulrich, M., Stark, S., Fuchs, M., Olofsson, J., Macias-Fauria, M., Kumpula, T. & Strauss, J. 2022c. *Peat and sediment characteristics from Reindeer winter ranges in Northern Finland* PANGAEA. doi:10.1594/PANGAEA.952470.

Windirsch, T., Forbes, B. C., Grosse, G., Wolter, J., Stark, S., Treat, C. C., Ulrich, M., Fuchs, M., Olofsson, J., Kumpula, J., Macias-Fauria, M. & Strauss, J. 2023c. *Impacts of reindeer on soil carbon storage in the seasonally frozen ground of northern Finland*. Boreal Environment Research https://www.borenv.net/BER/archive/pdfs/ber28/ber28-207-226.pdf.

Wynn, J. G. 2007. *Carbon isotope fractionation during decomposition of organic matter in soils and paleosols: Implications for paleoecological interpretations of paleosols*. Palaeogeography, Palaeoclimatology, Palaeoecology 251 (3): 437-448, doi:10.1016/j.palaeo.2007.04.009.

Ylänne, H., Olofsson, J., Oksanen, L. & Stark, S. 2018. *Consequences of grazer-induced vegetation transitions on ecosystem carbon storage in the tundra*. Functional Ecology 32 (4): 1091-1102, doi:10.1111/1365-2435.13029.

Zhang, C., Douglas, T. A., Brodylo, D. & Jorgenson, M. T. 2023. *Linking repeat lidar with Landsat products for large scale quantification of fire-induced permafrost thaw settlement in interior Alaska*. Environmental Research Letters 18 (1): 015003, doi:10.1088/1748-9326/acabd6.

Zimov, N. S., Zimov, S. A., Zimova, A. E., Zimova, G. M., Chuprynin, V. I. & Chapin III, F. S. 2009. *Carbon storage in permafrost and soils of the mammoth tundra-steppe biome: Role in the global carbon budget*. Geophysical Research Letters 36 (2) doi:10.1029/2008GL036332.

Zimov, S. A. 2005. *Pleistocene Park: Return of the Mammoth's Ecosystem*. Science 308 (5723): 796-798, doi:10.1126/science.1113442.

Zimov, S. A., Chuprynin, V. I., Oreshko, A. P., Chapin III, F. S., Reynolds, R. & Chapin, M. C. 1995. *Steppe-Tundra Transition: A Herbivore-Driven Biome Shift at the End of the Pleistocene*. The American Naturalist 146 (5): 765-794, doi:10.1086/285824.

975 **Tables**

976 Table 1 - Study sites in active layer (AL) and permafrost (PF) samples in permafrost-affected
977 soils in Cherskiy (CH), northeastern Siberia, from 2019, and in seasonally frozen ground
978 (SFG) in Finland (FI) from 2020 and 2022; grazing intensity defined from 1 (exclosure) to 5
979 (pasture).

Study area	site	sampling year	sampling size analysed	grazing intensity	ground thermal regime	soil type
Siberia	CH19-B1	2019	5	1	AL, PF	mineral, peat
	CH19-U1	2019	4	1	AL, PF	mineral
	CH19-B3	2019	4	3	AL, PF	mineral
	CH19-B5	2019	5	5	AL, PF	mineral, peat
	CH19-U5	2019	6	5	AL, PF	mineral
Finland	FI20-E-1M-A	2020	2	1	SFG	mineral
	FI22-E-1M-B	2022	1	1	SFG	mineral
	FI20-S-2M	2020	2	2	SFG	mineral
	FI22-S-2P	2022	1	2	SFG	peat
	FI20-S-3M	2020	2	3	SFG	mineral
	FI20-S-3P	2020	3	3	SFG	peat
	FI22-W-3P	2022	1	3	SFG	peat
	FI20-MR	2020	1	natural	SFG	mineral
	FI20-PR	2020	1	natural	SFG	peat
	FI22-W-4M	2022	1	4	SFG	mineral
	FI20-S-4P	2020	3	4	SFG	peat
	FI22-W-4P	2022	2	4	SFG	peat
	FI20-S-5M	2020	1	5	SFG	mineral
	FI22-W-5M	2022	1	5	SFG	mineral
	FI20-S-5P	2020	3	5	SFG	peat
	FI22-W-5P-A	2022	2	5	SFG	peat
	FI22-W-5P-B	2022	2	5	SFG	peat

FI20-S-5F	2020	3	5	SFG	peat

980

Figure captions

Figure 1 - Study site map indicating locations of all sampled sites; all detail maps are oriented with North up; a) Sampling sites at the Kutuharju Field Research Station, northern Finland; b) Reference sampling sites in northern Finland outside the Kutuharju Field Research Station; c) Sampling sites in Pleistocene Park, northeastern Siberia; d) Overview map showing the study areas and their position in the Arctic; E: Exclosure site, S: Reindeer summer range sites, W: Reindeer winter range sites, B: Drained thermokarst lake basin sites, U: Yedoma upland sites, M: Mineral soil sites, P: Peat sites; Numbers 1 to 5 state the grazing intensity (1: no grazing/exclosure to 5: intensive grazing/pasture/supplementary feeding site); imagery provided by ESRI; coordinate system: EPSG:4326 – WGS 84.

Figure 2 - Carbon and lipid biomarker characteristics for the uppermost 38 cm for exclosure sites (grey), occasional grazing (dark green) and pastures (light green); from top to bottom: distribution plots of total organic carbon content (TOC), bulk stable carbon isotopes ($\delta^{13}C$), *n*-alkane average chain length ($ACL_{23\text{-}33}$), carbon preference index ($CPI_{23\text{-}33}$) and higher-plant alcohol index (HPA); left column: active layers (top 38 cm) from permafrost study sites; right column: top 38 cm samples of sites with seasonally frozen ground; for better comparability values for the dung reference samples are added as triangles; the shaded area in $CPI_{23\text{-}33}$ and HPA indicates the relative degree of degradation (high degradation / more degraded molecules on the left).

Figure 3 - Boxplots of $ACL_{23\text{-}33}$, $CPI_{23\text{-}33}$ and HPA comparing all active layer samples (Siberia; orange), permafrost samples (Siberia; blue) and seasonally frozen ground sites (Finland; red); dots mark outliers (more than 1.5 box lengths away from the median); white numbers provide the number of samples included in each boxplot; the shaded area in $CPI_{23\text{-}33}$ and HPA indicates the relative degree of degradation (high degradation / more degraded molecules on the left).

1010 Figure 4 - Visualisation of the different grazing intensities examined in this manuscript, and
1011 their characteristics regarding (relative) animal density, vegetation, and thaw depth (at
1012 permafrost-affected sites).

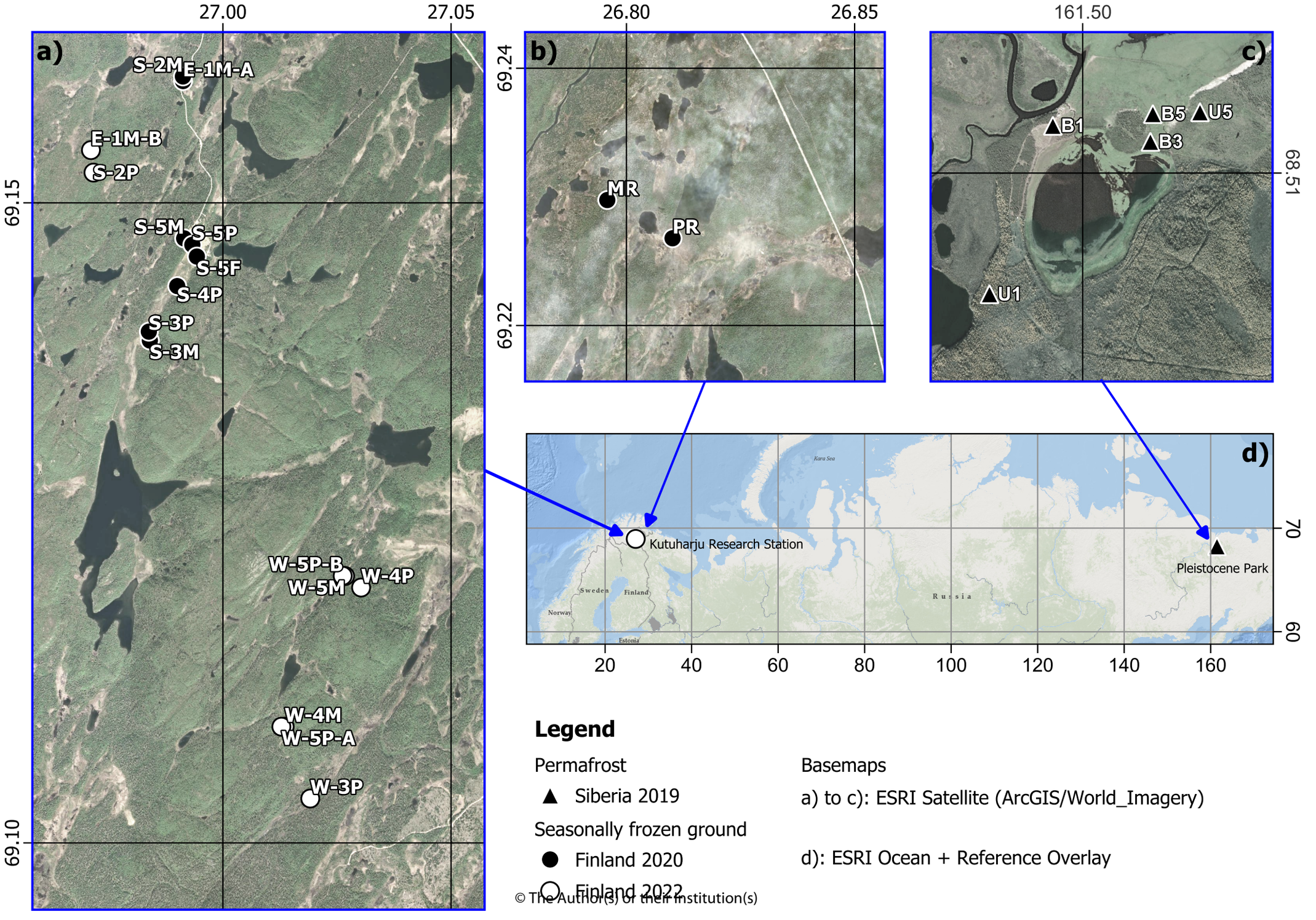

Legend

Permafrost

▲ Siberia 2019

Seasonally frozen ground

● Finland 2020

○ Finland 2022

Basemaps

a) to c): ESRI Satellite (ArcGIS/World_Imagery)

d): ESRI Ocean + Reference Overlay

uppermost 38 cm of every site

active layer on permafrost sites

seasonally frozen ground

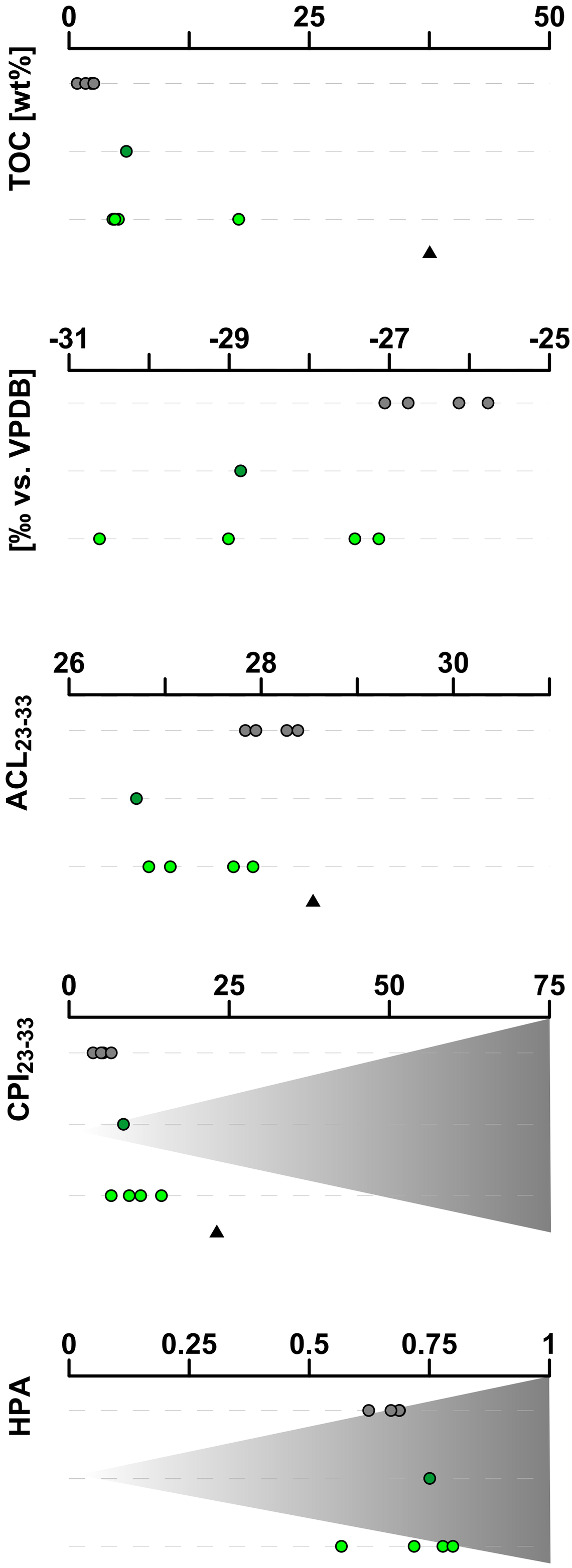

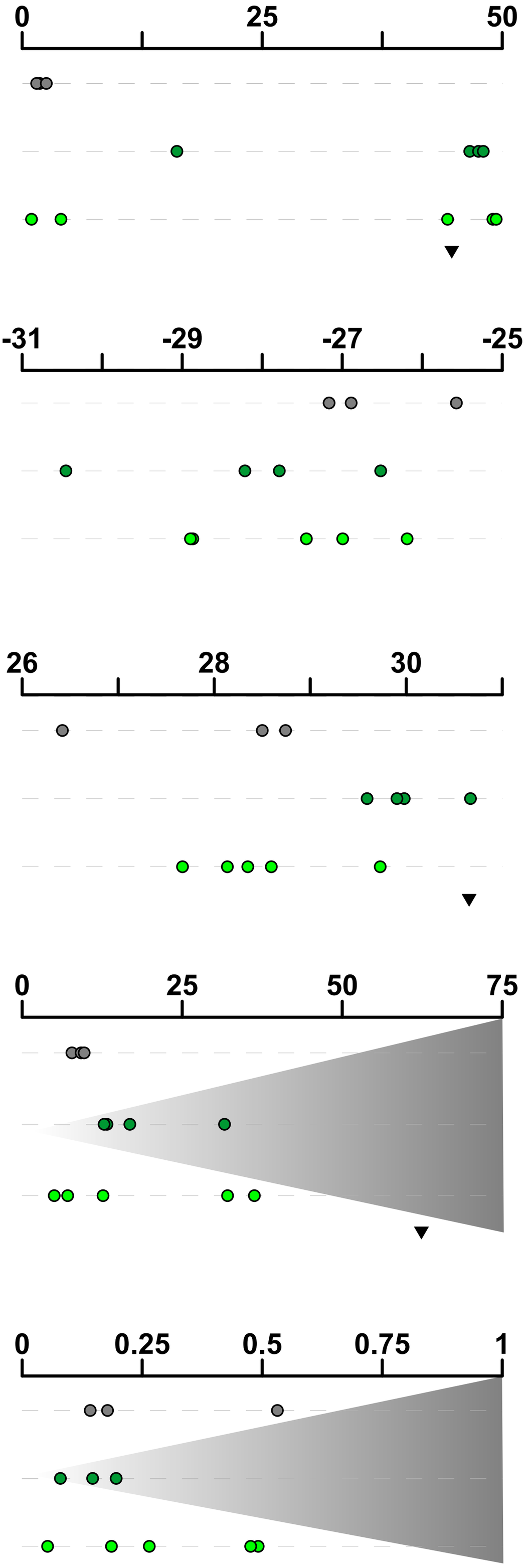

exclosure
occasional grazing
pasture

high relative degradation low

▲ horse dung
▼ reindeer dung

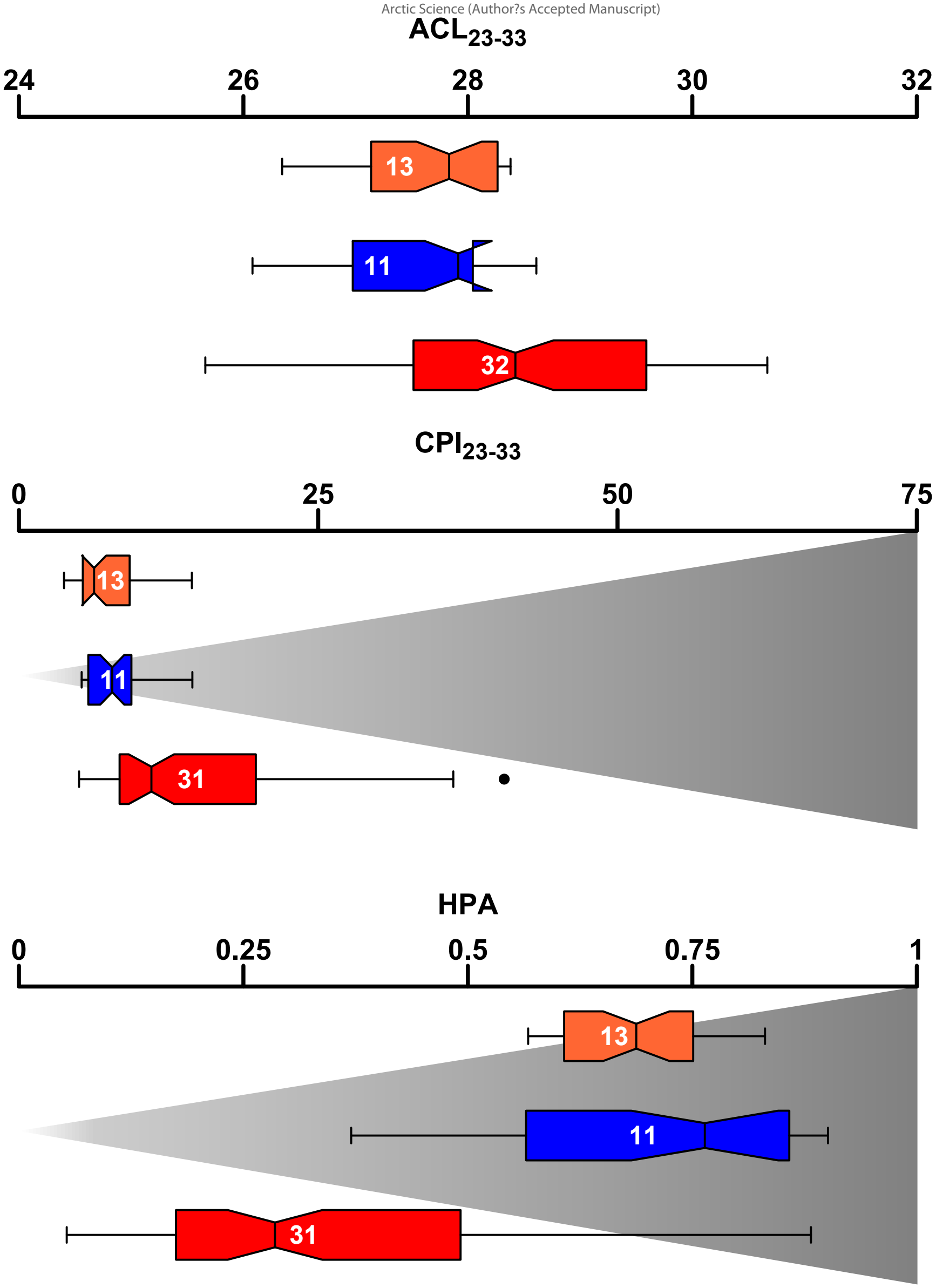

	intensity 1	intensity 3	intensity 5
setting	**exclosure**	**occasional grazing**	**pasture**
grazing		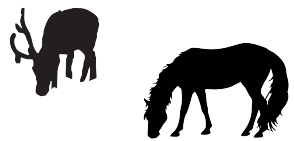	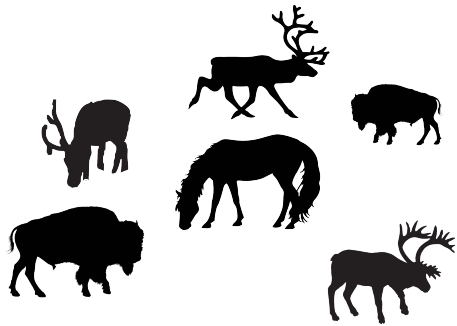
vegetation	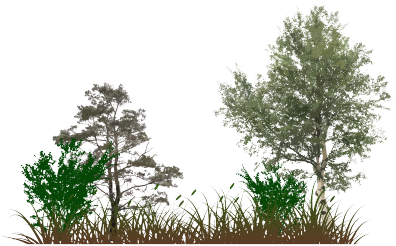 forest / shrub tundra	 tundra with shrubs	 grassland
thaw depth (to permafrost)	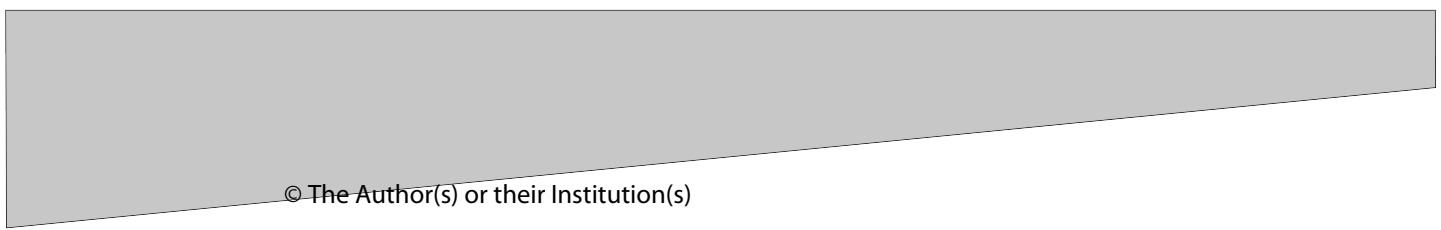 85 cm	55 cm	38 cm